Proceedings of the International Gas Turbine Congress 2003 Tokyo
November 2-7, 2003

IGTC2003Tokyo TS-054

Euler/N-S Analysis of Linear Unsteady Aerodynamic Forces on Vibrating Annular Cascade

Taketo NAGASAKI[1] and Nobuhiko YAMASAKI[1]

[1] Department of Aeronautics and Astronautics
Kyushu University
6-10-1 Hakozaki, Higashi-ku, Fukuoka 812-8581, JAPAN
Phone: +81-92-642-3730, FAX: +81-92-642-6752, E-mail: yamasaki@aero.kyushu-u.ac.jp

ABSTRACT

The paper presents the formulation to compute numerically the unsteady aerodynamic forces on the vibrating annular cascade blades in viscid and inviscid flows. The formulation is based on the finite volume method. By applying the TVD scheme to the linear unsteady calculations, the precise calculation of the peak of unsteady aerodynamic forces at the shock wave location like the delta function singularity becomes possible without empirical constants. As a further feature of the present paper, results of the present numerical calculation are compared with those of the double linearization theory (DLT), which assumes the inviscid flow with small unsteady and steady disturbances but the unsteady disturbances are much smaller than the steady disturbances. Since DLT requires far less computational resources than the present numerical calculations, the validation of DLT is quite important from the engineering point of view. Under the conditions of small steady disturbances, a good agreement between these two results is observed, so that the two codes are cross-validated. The comparison also reveals the limitation on the applicability of DLT. Also the extension of the method to the viscous flows are to be discussed and the numerical results are presented to compare the results.

INTRODUCTION

Precise numerical calculation of the unsteady aerodynamic forces on the vibrating cascade blades is highly required in relation to the flutter in turbomachines. To compute the unsteady inviscid flows and predict the unsteady aerodynamic forces on the vibrating cascade blades, there are two models, i.e., the linear (Hall, 1993), (Yamasaki, 2000) and non-linear unsteady aerodynamic models. The non-linear unsteady model requires a large amount of computational resources compared with the linear model (He, 1993) due to the time accurate calculation of the non-linear Euler equations. The linear unsteady model requires far less computational resources since it does not solve the non-linear Euler equations but solves the linearized Euler equations for the complex amplitude following the solution of the steady (time mean) Euler equations for the steady aerodynamic forces. In the flutter analysis of the cascade blades, the linear unsteady calculation is adequate because the aim of the analysis is not to calculate unsteady flows under deep flutter conditions of limit-cycle states but to predict the conditions susceptible to flutter by assuming small vibration amplitudes.

The authors' research group has developed the numerical method to calculate the linear unsteady flow field including shock waves with high accuracy using TVD scheme, and applied it to the two-dimensional supersonic through-flow fan blades in the inviscid unsteady supersonic flow to show the effectiveness of the method (Yamasaki, 2000). In extending the code to the three-dimensional annular geometry, we take advantage of using the rotating coordinate system version of UPACS code (Yamane, 2001) (Takaki, 2001) released for general use in 2000 by National Aerospace Laboratory (NAL), Japan. The steady or time-mean flow field is directly calculated by the UPACS code, and the linear unsteady field is calculated by the newly developed code which is developed from UPACS. The numerical methodology used in the linear unsteady calculation of the 2-D vibrating supersonic through-flow fan blades (Yamasaki, 2000) was the finite difference method and the non-MUSCL type. Following the numerical methodology used in UPACS, we reconstruct the linear unsteady formulation using the finite volume method, the MUSCL type, and the Cartesian coordinate (not the cylindrical coordinate). As a result especially the adoption of the Cartesian coordinate simplifies the formulation and coding, and the much part of the routines are developed quite easily from UPACS.

By the way, as a special technique to calculate unsteady aerodynamic forces on the vibrating blades under steady loadings the so-called double linearization theory (DLT) developed by the authors' research group is available. DLT is valid under the assumption that the steady and unsteady disturbances are small, and at the same time the unsteady disturbances are much smaller than the steady disturbances. It has been applied to various flow speed regimes and various geometrical configurations successfully, e.g., (Li, 1990), (Hanada, 1996). The crucial advantage of using DLT resides in that much smaller computational resources are required than the method based on the computational fluid dynamics (CFD). DLT program gives the 3-D unsteady pressure field in less than one second on current PCs. Since DLT assumes small steady disturbances, the present linear unsteady calculation based on CFD, which is free from the assumption of small steady disturbances, can be used for validation of DLT, too.

In the present paper, the CFD formulation using TVD and MUSCL, and the numerical results of linear unsteady aerodynamic forces on vibrating annular cascade blades, are presented. The present CFD results are compared with the DLT results, and the cross-validation of both methods as well as the limitation of the applicability of DLT are to be discussed.

NUMERICAL MODEL AND FORMULATION

Fundamental Equations

In the present paper, a single row of annular rotating blades as shown in Fig.1 is considered and the effects of the adjacent blade rows downstream and upstream are assumed to be negligible. Cascade blades are assumed to vibrate harmonically in infinitesimally small amplitude with a constant angular frequency

Manuscript Received on April 6, 2003

ω and a uniform interblade phase angle $2\pi\sigma$. Tip clearances are neglected. The hub and casing radii are assumed to be uniform in the present paper, but this assumption is not essential in the formulation. Fluid is the viscous or inviscid air ideal gas with the constant specific heat. Since the finite volume formulation is employed, the fundamental equation is satisfied in the control volumes. The rotating coordinate system which rotates at an angular velocity of $\mathbf{\Omega}$ with respect to the inertial coordinate system. The Navies-Stokes (N.S.) equations which govern the flow field at the position is given in the integral form in the rotating coordinate system.

$$\frac{\partial}{\partial t}\int_V \mathbf{Q}dV + \int_A \mathbf{F_c}\,dA + \int_A \mathbf{F_v} + \int_V \mathbf{S}dV = 0 \ . \qquad (1)$$

Here,

$$\mathbf{Q} = \begin{pmatrix} \rho \\ \rho u_i \\ e_r \end{pmatrix},\ \mathbf{F_c} = \begin{pmatrix} \rho u_j \\ \rho u_j u_i + p n_i \\ \rho u_j I \end{pmatrix},$$

$$\mathbf{F_v} = \begin{pmatrix} 0 \\ \tau_{ij} \\ \tau_{ij} u_i + \kappa \dfrac{\partial T}{\partial x_j} \end{pmatrix},\quad \mathbf{S} = \begin{pmatrix} 0 \\ \mathbf{f_1} + \mathbf{f_2} \\ 0 \end{pmatrix} \quad . \qquad (2)$$

And,

$$e_r = \frac{p}{\kappa - 1} + \frac{1}{2}\rho\ \mathbf{u}\cdot\mathbf{u} - \frac{1}{2}\rho(\Omega\times\mathbf{x})^2,\ U = \mathbf{n}\cdot\mathbf{u},$$

$$I = \frac{\kappa}{\kappa - 1}\frac{p}{\rho} + \frac{1}{2}\mathbf{u}\cdot\mathbf{u} - \frac{1}{2}(\Omega\times\mathbf{x})^2,$$

$$\mathbf{f_1} = 2\rho(\mathbf{\Omega}\times\mathbf{u}),\ \mathbf{f_2} = \rho\ \mathbf{\Omega}\times(\mathbf{\Omega}\times\mathbf{x})$$

Further, ρ is the fluid density, $\mathbf{u} = (u, v, w)$ is the relative speed of flow, e_r is the total energy per unit volume in the rotating coordinate system, p is the pressure, κ the specific heat ratio, I is the rothalpy in the rotating coordinate system corresponding to the enthalpy in the inertial coordinate system. $\mathbf{f_1}$ and $\mathbf{f_2}$ are the additional external forces of the Coriolis and centrifugal forces, respectively, due to the rotating coordinate system fixed to the rotating blades in use. dA and dV denote respectively the control surface and volume elements for integrals. The pressure p and the total energy per unit volume in the rotating coordinate system e_r are related by the equation,

$$p = (\kappa - 1)\left\{e_r - \frac{1}{2}\rho\mathbf{u}\cdot\mathbf{u} + \frac{1}{2}\rho(\mathbf{\Omega}\times\mathbf{x})^2\right\}$$

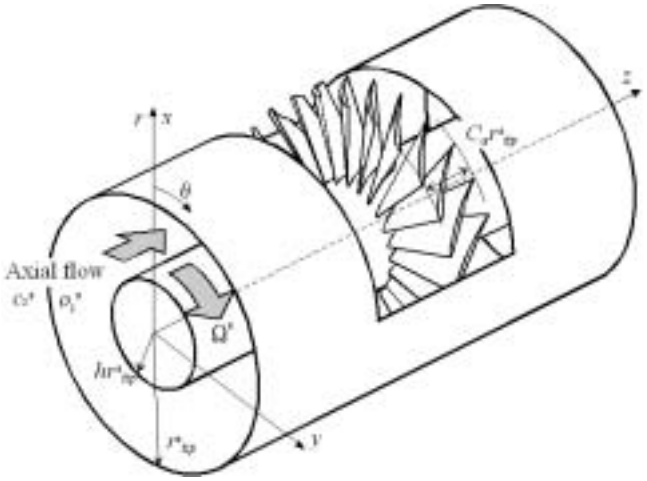

Fig. 1 Computational model and coordinate systems

Linear Unsteady N-S Equations

Next, the basic equation (1) is linearized under the assumption that the vibration amplitude is small enough so that the unsteady disturbances are small compared with the steady disturbances (Hall, 1993). Let us denote the time mean position of the blade by the intermediate coordinate system $(\overline{x}, \overline{y}, \overline{z}, t)$. In this intermediate coordinate system, the vibrating blades are assumed to be fixed. The x, y and z components of the small displacement amplitude of the blade are given respectively by $\tilde{x}(\overline{x}, \overline{y}, \overline{z})e^{i\omega t}$, $\tilde{y}(\overline{x}, \overline{y}, \overline{z})e^{i\omega t}$ and $\tilde{z}(\overline{x}, \overline{y}, \overline{z})e^{i\omega t}$. Then the coordinate transform of the physical coordinate (the rotating coordinate system fixed to the rotor) and the intermediate coordinate systems are given by

$$\begin{aligned} x &= \overline{x} + \tilde{x}(\overline{x}, \overline{y}, \overline{z})e^{i\omega t} \\ y &= \overline{y} + \tilde{y}(\overline{x}, \overline{y}, \overline{z})e^{i\omega t} \\ z &= \overline{z} + \tilde{z}(\overline{x}, \overline{y}, \overline{z})e^{i\omega t} \\ t &= t \end{aligned} \qquad (3)$$

In the following formulations, the superscripts $\overline{x}$ and $\tilde{x}$ denote the steady or time-mean part and the complex amplitude of the time fluctuating part, respectively.

Correspondingly, the flow field $\mathbf{Q}$ can be given by the superposition of the time-mean, i.e., steady flow field $\overline{\mathbf{Q}}$ and the first order perturbed flow field $\tilde{\mathbf{Q}}e^{i\omega t}$ due to vibration of the cascade blades of harmonic time dependence with a small amplitude. By retaining up to the first order terms, we obtain

$$
\begin{aligned}
\mathbf{Q}(x,y,z,t) &= \overline{\mathbf{Q}}(\overline{x},\overline{y},\overline{z}) + \tilde{\mathbf{Q}}(\overline{x},\overline{y},\overline{z},t)e^{i\omega t} \\
\mathbf{F_c}(x,y,z,t) &= \overline{\mathbf{F}}_{\mathbf{c}}(\overline{x},\overline{y},\overline{z}) + \tilde{\mathbf{F}}_{\mathbf{c}}(\overline{x},\overline{y},\overline{z},t)e^{i\omega t} \\
\mathbf{F}_v(x,y,z,t) &= \overline{\mathbf{F}}_v(\overline{x},\overline{y},\overline{z}) + \tilde{\mathbf{F}}_v(\overline{x},\overline{y},\overline{z},t)e^{i\omega t} \\
\mathbf{S}(x,y,z,t) &= \overline{\mathbf{S}}(\overline{x},\overline{y},\overline{z}) + \tilde{\mathbf{S}}(\overline{x},\overline{y},\overline{z},t)e^{i\omega t}
\end{aligned} \tag{4}
$$

Here

$$
\tilde{\mathbf{F}}_{\mathbf{c}} = \frac{\partial \overline{\mathbf{F}}_{\mathbf{c}}}{\partial \overline{\mathbf{Q}}}\tilde{\mathbf{Q}}, \quad \tilde{\mathbf{F}}_v = \frac{\partial \overline{\mathbf{F}}_v}{\partial \overline{\mathbf{Q}}}\tilde{\mathbf{Q}}, \quad \mathbf{S} = \frac{\partial \mathbf{S}}{\partial \overline{\mathbf{Q}}}\tilde{\mathbf{Q}} \tag{5}
$$

Substituting Eq.(3) into Eq.(1) and retaining up to the first order terms, we can decompose it into the steady part

$$
\frac{\partial}{\partial t}\int_{\overline{V}} \overline{\mathbf{Q}} d\overline{V} + \int_{\overline{A}} \overline{\mathbf{F}} d\overline{A} + \int_{\overline{V}} \overline{\mathbf{S}} d\overline{V} = 0 \tag{6}
$$

and the unsteady part

$$
\begin{aligned}
\frac{\partial}{\partial t}\int_{\overline{V}} \tilde{\mathbf{Q}} d\overline{V} + \int_{\overline{A}} (\tilde{\mathbf{F}}_c - \tilde{\mathbf{F}}_{\mathbf{b}} + \tilde{\mathbf{F}}_v) d\overline{A} + \int_{\overline{V}} (i\omega\tilde{\mathbf{Q}} + \tilde{\mathbf{S}}) d\overline{V} \\
= -\int_{\tilde{V}} (i\omega\overline{\mathbf{Q}} + \overline{\mathbf{S}}) d\tilde{V} - \int_{\tilde{A}} (\overline{\mathbf{F}}_c + \overline{\mathbf{F}}_v) d\tilde{A}
\end{aligned} \tag{7}
$$

Here

$$
\tilde{\mathbf{Q}} = \begin{pmatrix} \tilde{\rho} \\ \overline{\rho}\tilde{u}_i + \tilde{\rho}\overline{u}_i \\ \tilde{e}_r \end{pmatrix},
$$

$$
\tilde{\mathbf{F}}_c = \begin{pmatrix} \overline{\rho}\tilde{u}_j + \tilde{\rho}\overline{u}_j \\ \overline{\rho}\tilde{u}_j\tilde{u}_i + \tilde{\rho}\overline{u}_j\tilde{u}_i + \overline{\rho}\tilde{u}_j\overline{u}_i + \overline{n}_i\tilde{p} \\ \overline{\rho}\tilde{u}_j\tilde{I} + \tilde{\rho}\overline{u}_j\tilde{I} + \overline{\rho}\tilde{u}_j\overline{I} \end{pmatrix}, \tag{8}
$$

$$
\tilde{\mathbf{S}} = \begin{pmatrix} 0 \\ \tilde{\mathbf{f}}_1 + \tilde{\mathbf{f}}_2 \\ 0 \end{pmatrix}
$$

and

$$
\tilde{e}_r = \frac{\tilde{p}}{\kappa - 1} + \frac{1}{2}\tilde{\rho}\overline{\mathbf{u}}\cdot\overline{\mathbf{u}} + \overline{\rho}\mathbf{u}\cdot\tilde{\mathbf{u}} - \frac{1}{2}\tilde{\rho}\left(\Omega\times\mathbf{x}\right)^2, \quad \tilde{U} = \overline{\mathbf{n}}\cdot\tilde{\mathbf{u}},
$$

$$
\tilde{I} = \frac{\kappa}{\kappa - 1}\frac{1}{\overline{\rho}^2}\left(\tilde{p}\overline{\rho} + \overline{p}\tilde{\rho}\right) + \overline{\mathbf{u}}\cdot\tilde{\mathbf{u}},
$$

$$
\tilde{\mathbf{f}}_1 = 2\tilde{\rho}(\mathbf{\Omega}\times\overline{\mathbf{u}}) + 2\overline{\rho}(\mathbf{\Omega}\times\tilde{\mathbf{u}}), \quad \tilde{\mathbf{f}}_2 = \tilde{\rho}\mathbf{\Omega}\times(\mathbf{\Omega}\times\mathbf{x})
$$

$$
\tilde{p} = \left(\kappa - 1\right)\left\{\tilde{e}_r - \frac{1}{2}\tilde{\rho}\quad \overline{\mathbf{u}}\cdot\overline{\mathbf{u}} - \overline{\rho}\quad \overline{\mathbf{u}}\cdot\tilde{\mathbf{u}} + \frac{1}{2}\tilde{\rho}\left(\mathbf{\Omega}\times\mathbf{x}\right)^2\right\}
$$

Here $d\tilde{S}$ and $d\tilde{V}$ denote the complex amplitudes of time-varying surface and volume elements, respectively, for the integration. In Eq.(8), the terms

$$
\tilde{\mathbf{F}}_{\mathbf{b}} = \overline{\mathbf{Q}}\tilde{U}_b, \quad \tilde{U}_b = \overline{\mathbf{n}}\cdot\tilde{\mathbf{u}}_{\mathbf{b}} \tag{9}
$$

denote the additional flux due to the effect of displacement of the cell boundary surface at the velocity $\tilde{\mathbf{u}}_{\mathbf{b}}$ .Here $d\tilde{S}$ and $d\tilde{V}$ denote the complex amplitudes of time-varying surface and volume elements, respectively, for the integration. In Eq.(6), the terms

$$
\tilde{\mathbf{F}}_{\mathbf{b}} = \overline{\mathbf{Q}}\tilde{U}_b, \quad \tilde{U}_b = \overline{\mathbf{n}}\cdot\tilde{\mathbf{u}}_{\mathbf{b}} \tag{10}
$$

denote the additional flux due to the effect of displacement of the cell boundary surface at the velocity $\tilde{\mathbf{u}}_{\mathbf{b}}$.

Boundary Conditions

As the inflow and outflow boundary conditions, the non-reflecting boundary conditions which take into account the wave components are used. For the steady disturbances, the boundary conditions are formulated in terms of the Riemann invariants following the UPACS code, and for the unsteady disturbances, the boundary conditions are implemented following the unsteady 1-D formulation by Giles (Giles, 1990).

The slip boundary conditions which imply the inviscid flow moves smoothly on the blade surface are given by

$$
\mathbf{u}_{rel}\cdot\mathbf{n} = 0 \tag{11}
$$

Or the non-slip boundary conditions for the viscous flows given by

$$
\mathbf{u}_{rel} = 0
$$

are used. Here

$$
\mathbf{u}_{rel} = \mathbf{u} - \mathbf{u}_{blade} \tag{12}
$$

and $\mathbf{u}_{blade}$ and $\mathbf{u}_{rel}$ denote respectively the velocity of the blade surface and the relative velocity of the flow with respect to the blade surface. By retaining the terms up the first order, Eq. (11) is reduced to

$$
\overline{\mathbf{u}}\cdot\overline{\mathbf{n}} = 0 \tag{13}
$$

for steady components, and

$$
\tilde{\mathbf{u}}\cdot\overline{\mathbf{n}} = -\overline{\mathbf{u}}\cdot\tilde{\mathbf{n}} + \tilde{\mathbf{u}}_{blade}\cdot\overline{\mathbf{n}} \tag{14}
$$

for unsteady components. For the hub and casing walls which do not vibrate, also the slip conditions are applied.

In the present linear unsteady calculation, a single passage of the annular cascade blades is to be calculated by applying the periodicity in the circumferential direction. Thus for the circumferential boundaries, the periodical conditions

$$
\overline{\mathbf{Q}}(r,\theta+2\pi/N,z) = \overline{\mathbf{Q}}(r,\theta,z) \tag{15}
$$

for steady components, and

$$
\tilde{\mathbf{Q}}(r,\theta+2\pi/N,z) = \tilde{\mathbf{Q}}(r,\theta,z)e^{i2\pi\sigma} \tag{16}
$$

for unsteady components, are satisfied.

Details of Numerical Calculation

Since the finite volume formulation is used, the straight-forward

calculation on the physical intermediate Cartesian coordinate in stead of the numerical coordinate is executed following UPACS, released for general use in 2000 by National Aerospace Laboratory (NAL), Japan. In the time integration, the matrix-free Gauss-Seidel method for the steady calculations, and the Runge-Kutta-3rd method for the unsteady calculations, are used. In the evaluation of the volumes or the surface areas, the conventional method is used following UPACS for the steady calculation. This procedure is extended to evaluate the perturbation of the volumes or the surface areas by taking the linear unsteady amplitude of the volume and surface area. The evaluation of the convective terms, the MUSCL formulation, and the evaluation of the eigen-vectors follow the method used in UPACS.

As for the unsteady calculation procedures, the TVD scheme initially applied to the non-MUSCL formulation and the finite difference method (Yamasaki, 2000) is extended to the MUSCL formulation and the finite volume method.

The implementation of the MUSCL formulation and the TVD scheme in the linear unsteady calculations are to be outlined next. In MUSCL method, the distribution of the physical properties in the grid cells are approximated by the piecewise constant, first-, or second-order polynomial distribution.

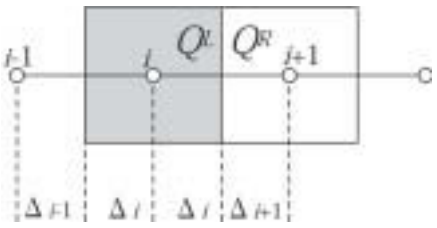

Fig. 2 Grid points

By using the grid cell width Δ given in Fig. 2, the physical properties $\tilde{\mathbf{Q}}$ are given by

$$\tilde{\mathbf{Q}}_{i\pm1/2} = \tilde{\mathbf{Q}}_i \pm \frac{1}{2}\left[(1\pm\lambda)\tilde{\mathbf{Q}}'_{i+1/2} + (1\mp\lambda)\tilde{\mathbf{Q}}'_{i-1/2}\right] \tag{17}$$

where

$$\tilde{\mathbf{Q}}'_{i+1/2} = \frac{\tilde{\mathbf{Q}}_{i+1} - \tilde{\mathbf{Q}}_i}{\Delta_{i+1} + \Delta_i}, \tilde{\mathbf{Q}}'_{i-1/2} = \frac{\tilde{\mathbf{Q}}_i - \tilde{\mathbf{Q}}_{i-1}}{\Delta_i + \Delta_{i-1}}. \tag{18}$$

In the present linear unsteady calculations, $\lambda = 1/3$ (third-order accurate) is adopted. The TVD scheme is applied to limit $\tilde{\mathbf{Q}}'_{i+1/2}$ and $\tilde{\mathbf{Q}}'_{i-1/2}$ by using the cminmod limiter, which is the extension of the minmod limiter for the non-complex numbers,

$$\tilde{\mathbf{Q}}'_{i+1/2} = \min\text{mod}(\tilde{\mathbf{Q}}'_{i+1/2}, \overline{\omega}_- \tilde{\mathbf{Q}}'_{i-1/2})$$

$$\tilde{\mathbf{Q}}'_{i-1/2} = \min\text{mod}(\tilde{\mathbf{Q}}'_{i-1/2}, \overline{\omega}_+ \tilde{\mathbf{Q}}'_{i+1/2})$$

where

$$\overline{\omega}_\pm = \frac{1}{1-\lambda}\left(1+\lambda+2\frac{\Delta_{i\pm1}}{\Delta_i}\right)$$

and

$$\text{cminmod}(x, y) = \text{cmplx}(\text{minmod}(\text{real}(x), \text{real}(y)), \text{minmod}(\text{imag}(x), \text{imag}(y)))$$

Here $\text{real}(x)$, $\text{imag}(x)$ and $\text{cmplx}(x, y)$ denote the real part, imaginary part, and complex number conversion, respectively.

The vibration displacement vector can be given arbitrary in space as far as the specified displacement on the blade surface is satisfied. Details on the vibration displacement vector are omitted here due to the limited space of the paper. The calculation is implemented using non-dimensional numbers following the implementation in UPACS. The numerical grid points are generated by the Gridgen software by Pointwise Inc..

RESULTS AND DISCUSSION

Euler Calculation Results and Their Comparison with DLT

In the present paper, the unsteady aerodynamic forces of the rotating annular blades are calculated by using the numerical methods based on the computational fluid dynamics (CFD) outlined so far, and are discussed mainly in conjunction with the comparison with the double linearization theory (DLT). We should note again here that in DLT, the steady disturbances are assumed to be small, while, no such assumption is required, i.e., the steady disturbances may remain finite, in the present CFD formulation.

In the following calculations, the number of blades is fixed to $N = 60$, the hub/casing diameter ratio $h = 0.7$, and the non-dimensional axial chord length using the casing radius $C_a = 0.2$. Furthermore, the non-dimensional rotating speed is fixed to $\Omega = 0.197$, the non-dimensional angular frequency $\omega = 0.04$ for the present cases with the subsonic axial velocity. The blade geometrical profile, the time-mean angle of attack α ,the time-mean inflow axial Mach number M_a, and the interblade phase angle $2\pi\sigma$ are varied in the following calculations. Here, the non-dimensional quantities are non-dimensionalized using the casing radius, the stagnation speed of sound of the main flow, and the stagnation density of the main flow. Only the angular, i.e., torsional, vibration is considered, and the elastic axis is at the mid-chord in all calculations. The number of the grid points are, 21 in the spanwise (radial) direction, 21 in the circumferential direction, 141 in the axial direction of the annular duct, and 61 axial grid points are included in the bladed part of the annular duct for the inviscid calculations.

The steady and unsteady pressures shown below are both non-dimensionalized by $\rho_s c_s^2/2$ .The linear unsteady pressure is that per the vibrating rotating amplitude of one radian at the tip. Here c_s and ρ_s denote respectively the speed of sound and density at the stagnation condition of the main flow. Also the radial and axial positions are non-dimensionalized by the casing radius. In the figures, LT denotes the linear theory for the steady calculations, DLT denotes the double linearization theory for unsteady calculations, and CFD denotes the present linear unsteady calculation based on CFD.

Cascade blades with a subsonic relative flow

At first, let us consider the cascade blades with a small angle of attack of $\alpha = 2$ degrees, no camber and no thickness, placed in an inviscid subsonic flow with the axial Mach number of $M_a = 0.4$, and undergoing the torsional vibration. Note that the relative flow

around the blades is subsonic everywhere along the span. Figure 3 shows the non-dimensional steady pressure distributions by the present non-linear calculation based on the computational fluid dynamics (CFD) and by the linear theory based on the singularity method which is the steady part of the double linearization theory (DLT) (Namba, 1972). Figure 4 shows the non-dimensional linear unsteady pressure distributions at the interblade phase angle of $2\pi\sigma = 90$ degrees, by the present calculation based on CFD and by the calculation based on DLT (Li,1990). The horizontal axes in both figures are the position on the blade non-dimensionalized by using the outer casing radius of the double annular duct.

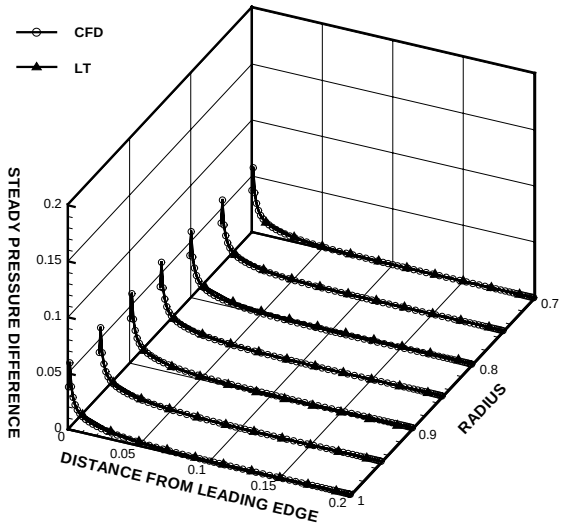

Fig. 3 Steady pressure difference distribution. AOA = 2 deg. parabolic blade with no camber and no thickness.

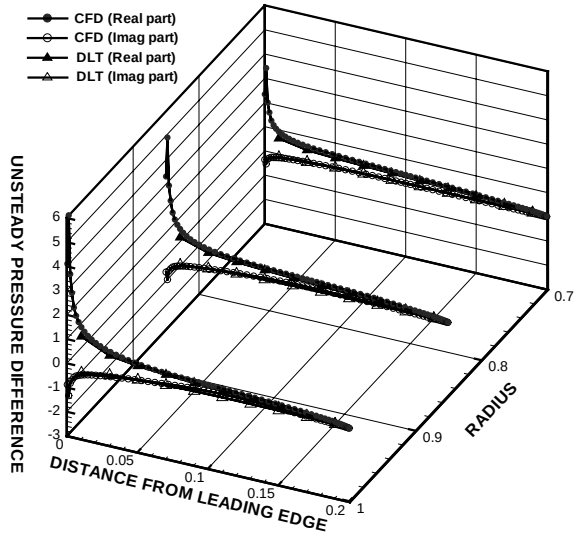

Fig. 4 Unsteady pressure difference distribution. AOA = 2 deg. parabolic blade with no camber and no thickness, $2\pi\sigma$ =90deg., ω =0.04.

Since the steady disturbance is small, little difference is observed between the present calculation and DLT in the steady and unsteady pressure distributions as is shown in Figs 3 and 4 respectively. Due to the limited space of the paper, the figures are omitted, but it is confirmed, for every interblade phase angles, a good agreement is observed between the present calculation based on CFD and the calculation based on DLT.

Parameter: Angle of Attack

Figure 5 shows the unsteady pressure difference on the airfoil at the various angle of attack from 2 degrees to 8 degrees. The camber ratio and the thickness ratio are fixed to 3% and 3%, respectively. The interblade phase angle is also fixed to 90 degrees. The Euler calculations and the DLT results show good agreement as much as the angle of attack of 8 degrees. Figure 6 shows the non-dimensional spanwise aerodynamic work of the blade at various angle of attack. In the DLT results, the effect of the angle of attack on the aerodynamic work is linear, and it is found its effect is small as is seen in Fig. 6. The Euler calculations, on the other hand, show the relatively large dependence on the angle of attack. At the present condition, it is found that the larger the angle of attack , the more close the Euler calculation and the DLT results, but this tendency should not be the general one.

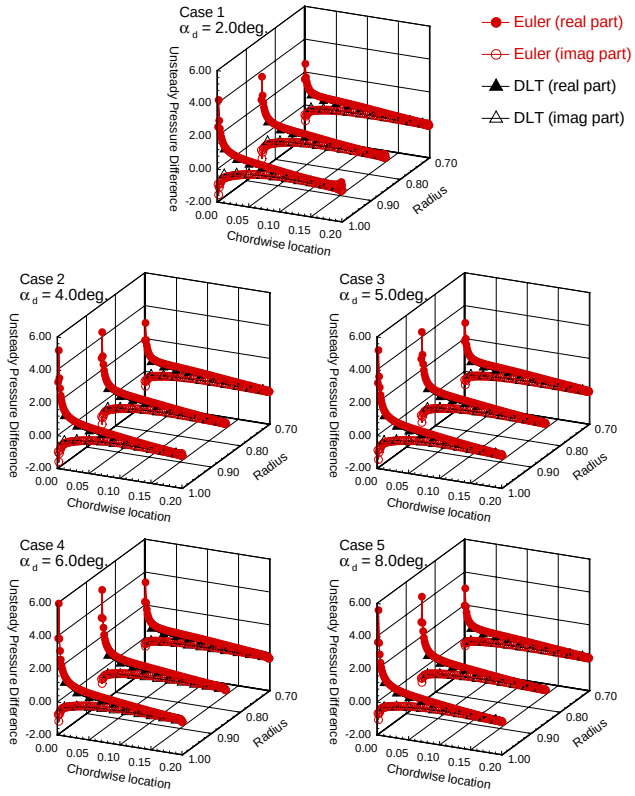

Fig.5 Unsteady pressure difference distribution. AOA = 2,4,5,6,8 deg. parabolic blade with 3% camber and 3% thickness, $2\pi\sigma$ =90deg., ω =0.04.

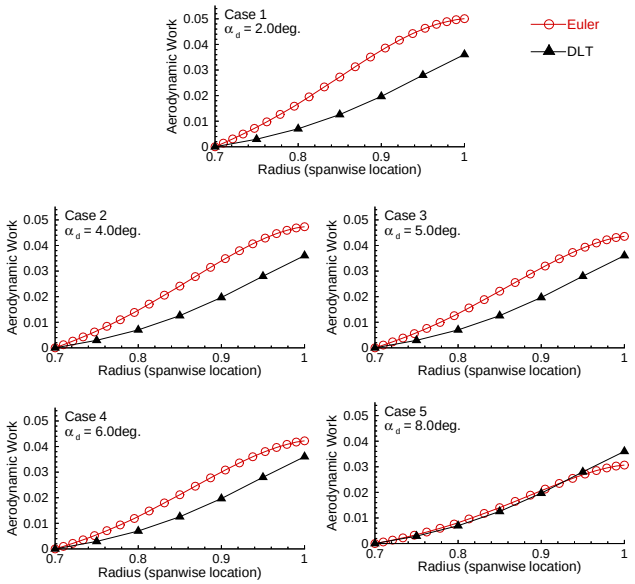

Fig.6 Unsteady spanwise aerodynamic work along spanwise direction. AOA = 2,4,5,6,8 deg. (parabolic blade with 3% camber and 3% thickness, $2\pi\sigma$ =90deg., ω =0.04)

Parameter : IBPA (Inter Blade Phase Angles)

Figure 7 shows the spanwise aerodynamic work for various interblade phase angle. Since the imaginary part of the moment corresponds to the aerodynamic work, the aerodynamic work becomes small at the interblade phase angles of 0 and 180 degrees. Figure 8 shows the total aerodynamic work for various interblade phase angle. Note the total aerodynamic work is the integration of the spanwise aerodynamic work shown in Fig. 7. Also one should note that the aerodynamic work for the pure torsional vibration as is in the paper, aerodynamic work is closely related to the imaginary part of the aerodynamic moment, so the tendency of the unsteady pressure and aerodynamic work on parameters may different. The DLT prediction gives about 0.75 times smaller value compared with the Euler calculations. This is due to the difference in the handling of the boundary conditions, and in the assumption on the effect of the steady disturbance on the unsteady disturbances, in the assumption on the steady disturbance etc. More specifically, the handling of the boundary conditions refers the followings: In the DLT formulation, the uniform axial Mach number and the pressure are stipulated upstream. On the other hand, in the Euler calculations, the upstream Mach number is determined so that the pressure condition at the downstream boundary is satisfied. Author's calculation (Nagasaki, 2003) indicates that the difference of the DLT prediction and the Euler results becomes smaller when the stagger angle is smaller.

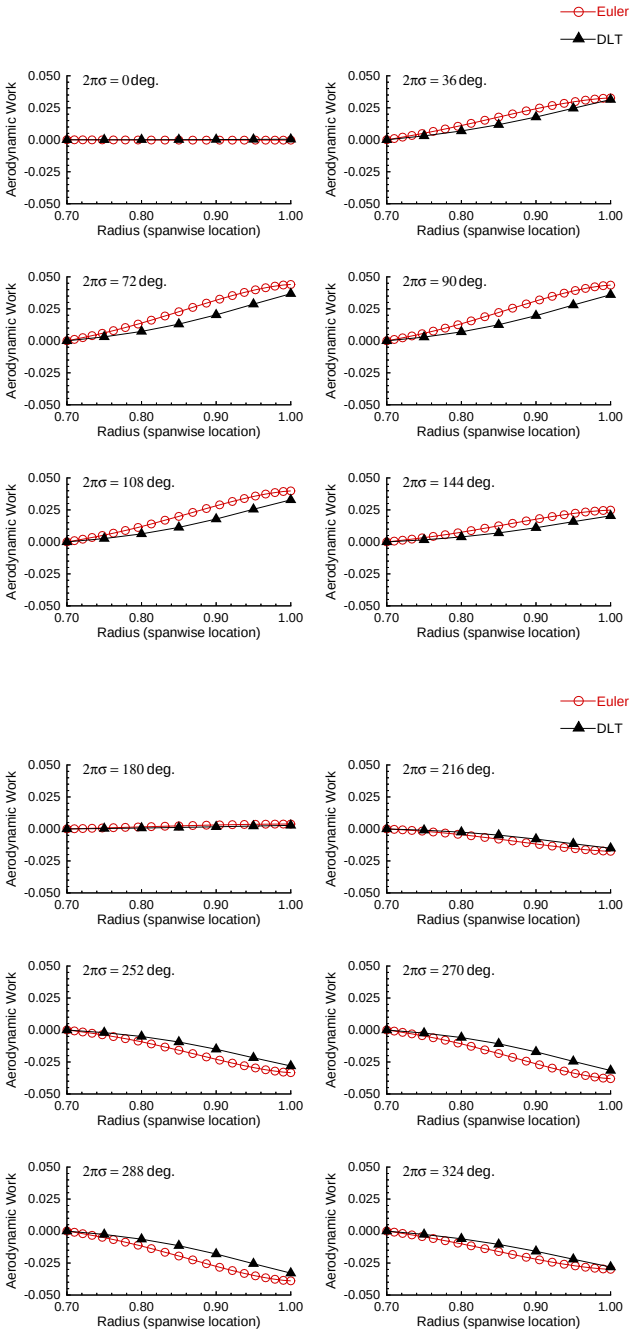

Fig. 7 Unsteady spanwise aerodynamic work. (parabolic blade with 3% camber and 3% thickness, $2\pi\sigma$ =0~360deg., ω =0.04)

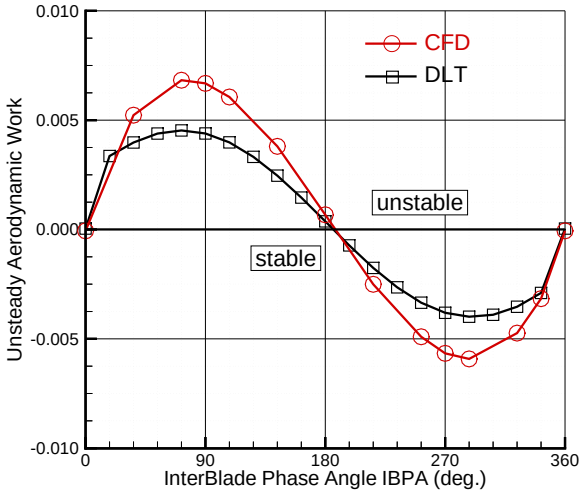

Fig.8 Unsteady total aerodynamic work. (parabolic blade with 3% camber and 3% thickness, $2\pi\sigma$ =0~360deg., ω =0.04)

Navier-Stokes Calculation Results and Ther Comparison with DLT

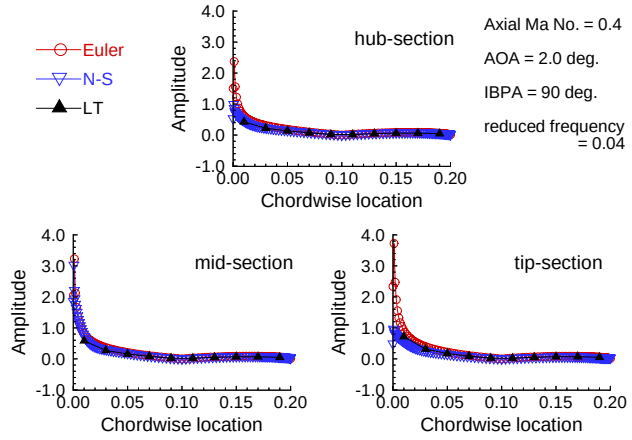

Fig.9 Amplitude of unsteady torsional moment at various span section. (flat plate with no camber and no thickness, $2\pi\sigma$ =90deg., ω =0.04)

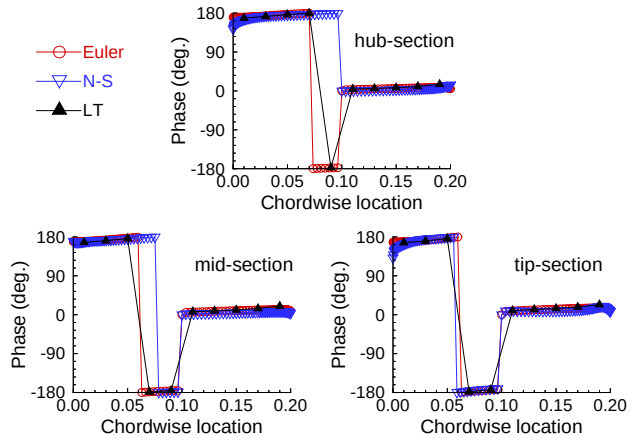

Fig.10 Phase of unsteady torsional moment at various span section.

(flat plate at the angle of attack of 2 degrees with no camber and no thickness, $2\pi\sigma$ =90deg., ω =0.04)

At last the linear Euler and Navier-Stokes calculations are compared. Figure 9 and 10 show the amplitude and phase of the unsteady torsional moment at various span section for the flat plate blade at the angle of attack of 2 degrees with no camber and no thickness. Because the effects of viscosity are large near the wall, the difference between the Euler and Navier-Stokes calculations becomes more conspicuous near the hub and casing. The Navier-Stokes calculations predict smaller moment than the Euler calculations, but their difference is not so large. As for the total non-dimensional aerodynamic work is concerned, $W_{\text{Euler}} = 5.5\times10^{-5}$, $W_{\text{NS}} = 4.9\times10^{-5}$ and $W_{\text{DLT}} = 4.5\times10^{-5}$ are obtained. As far as the Mach number is small and the steady disturbances are small so that no separation is present, the Euler calculations as well as the DLT calculations give rise to the qualitatively sufficient predictions correspondent with the Navier-Stokes calculations.

CONCLUSION

In the present paper, the model of a single row of annular rotating cascade blades is analyzed by the computational fluid dynamics (CFD). The linear unsteady aerodynamic flows around the vibrating blades which should be superimposed on the steady flow are calculated. In the steady aerodynamic calculations, the non-linear Euler or Navier-Stokes equations are solved, and in the linear unsteady aerodynamic calculations, the linear unsteady Euler or Navier-Stokes equations which determine the magnitude and phase of the unsteady components are solved, by using the finite volume method and the MUSCL formulation. Also the TVD scheme which is known to suppress the oscillation around the shock waves and to have few parameters determined empirically has successfully applied. The main conclusions obtained are as follows:

- When the steady disturbances are small and the relative flow is subsonic, the results of the present method based on Euler equations correspond well with those of the double linearization theory (DLT). So the present code based on the the Euler equations and the DLT codes are cross-validated with each other. The dependence of the aerodynamic forces on the interblade phase angle shows the same tendency between the Euler calculations and DLT.

- When the relative flow is subsonic but the steady disturbance is large, the results of the present method based on CFD show difference from the results of the linear theory in the steady flow field. The Euler calculations and the DLT results show good agreement as much as the angle of attack of 8 degrees. In the DLT results, the effect of the angle of attack on the aerodynamic work is linear, and it is found its effect is small. The Euler calculations, on the other hand, show the relatively large dependence on the angle of attack.

- As far as the axial Mach number is low and the steady disturbances are low, the numerical results by the Navier-Stokes equations agree well with the numerical results by the Euler equations except near the side wall where the small difference is observed. Thus the effect of viscosity is relatively small for such low Mach number and low steady disturbance flows. Alternatively the DLT also can predict the low Mach number and low steady unsteady disturbance flows.

Authors would like to acknowledge Dr. Kazuomi Yamamoto, National Aerospace Laboratory, Japan, for providing them with the technical advice on the usage of UPACS and for the fruitful discussion.

REFERENCES

Giles, M.B., 1990, “Non-reflecting Boundary Conditions for Euler Equation Calculations,” AIAA Journal, Vol.28, No. 12, pp.2050-2058.

Giles, M.B., 1988, “Non-reflecting Boundary Conditions for the Euler Equations,” Computational Fluid Dynamics Lab. TR 195, MIT.

Hall, K.C., 1993, “Linearized Euler Predictions of Unsteady Aerodynamic Loads in Cascades,” AIAA Journal, Vol. 31, No. 3, pp.540-550.

Hanada, T., and Namba, M., 1996, “Unsteady Aerodynamic Analysis of Supersonic Trough-Flow Fan with Vibrating Blades under Non-Zero Mean Loading,” Journal of Sound and Vibration, VOL.194, No. 5, pp.709-750.

He, L., and Denton, J.D., 1993, “Inviscid-Viscous Coupled Solution for Unsteady Flows Through Vibrating Blades: Part1 -Description of the Method,” ASME Journal of Turbomachinery, Vol.115, pp.94-100.

Hirsch, C., 1988, “Numerical Computation of Internal and External Flows, Vol. 1, Fundamentals of Numerical Discretization,” John Wiley & Sons.

Li, P., Toshimitsu, K., and Namba, M., 1990, “Double Linearization Theory for a Rotating Subsonic Annular Cascade of Oscillating Blades (Part 1, Mathematical Expressions of Disturbance Flow Field and Part 2, Numerical Study of Unsteady Aerodynamic Forces),” Memoirs of the Faculty of Engineering, Kyushu University, Vol.50, No.2, pp.161-199.

Namba, M., 1972, “Lifting Surface Theory for a Rotating Subsonic or Transonic Blade Row,” ARC Reports and Memoranda, No.3740.

Nagasaki, T,. 2003, “Euler/NS Analysis of Linear Unsteady Aerodynamic Forces on Vibrating Annular Cascade,” Master Thesis, Department of Aeronautics and Astronautics, Kyushu University.

Sbardella.L., and Imregun, M., 2001, ”Linearized Unsteady Viscous Turbomachinery Flows Using Hybrid Grids,” Journal of Turbomachinery, Vol.123, pp568-582.

Takaki, R., Yamamoto, K., Yamane, T., Enomoto, S., Makida, M., Yamazaki, H., Iwamiya, T., and Nakamura, T., 2001, “Current status of CFD platform - UPACS -},” Proceedings of International Parallel CFD 2001 Conference.

Yamane, T., Yamamoto, K., Enomoto, S., Yamazaki, H., Takaki, R., and Iwamiya, T., 2001, “ Development of a Common CFD Platform -UPACS-},” Proceedings of the Parallel Computational Fluid Dynamics 2000 Conference, pp257-264, Elsevier Science B.V.

Yamasaki, N., and Namba, M., 2000, “Unsteady Aerodynamics Forces on Vibrating Supersonic Through-Flow Fan Blades”, Proceedings of 9th International Symposium on Unsteady Aerodynamics, Aeroacoustics and Aeroelasticity of Turbomachines and First Legedre Lecture Series.